Effect of Aging on Oxidation Behavior of Aluminum-Albite Composites at High Temperatures

S.C. Sharma

(Submitted 29 September 1999; in revised form 3 February 2000)

The oxidation behavior of an aluminum composite reinforced with albite particles of 1, 2, 3, and 4 wt.% at 500 to 800 K has been investigated. Within the experimental temperature range, a parabolic weight change/area was observed with activation energy. The weight change/area as a function of oxidation time becomes linear after an initial period. On oxidation, formation of an oxide scale was found whose morphology depends on temperature, cooling rate, and subscale formation at the interface between the matrix and reinforcement. Detailed analysis by scanning electron microscopy (SEM) showed that the oxide scales were not homogenous throughout, but exhibited several layers, which differ in microstructure and composition with an increase in thickness. The presence of albite particulate reinforcement significantly affects the oxidation behavior. The interface oxidization kinetics was found to be higher than that in the other regions. The oxidation products were both metallic oxides and their respective alloying element oxides. The exposure time of specimens to oxidation was 1000 min, chosen to study oxidation behavior at different temperatures. The aging of both matrix and composite specimens improves oxidation resistance due to the residual stress-relaxation phenomena accompanying these specimens.

Keywords	aluminum alloys, aluminum alloy 6061, environmental effects, oxidation, metal matrix composites

1. Introduction

Metal matrix composites (MMCs) reinforced with ceramic particulates, whiskers, or fibers have received increasing attention due to their potentially high fracture toughness and strength.[1–5] Particle reinforced aluminum MMCs find potential applications in several thermal environments, especially in automobile engine parts, such as drive shafts, cylinders, pistons, and brake rotors, [6] and in space applications. With the exception of gold, no metal and alloy is stable in air at room temperature, which tend to form oxides. Most metals in the solid or liquid state are morphologically unstable in air at any temperature. An investigation relating to the temperature profiles of the piston area in a diesel engine has shown that the temperature can reach as high as 200 to 600 °C in certain regions.[7] As the piston and cylinder areas are exposed to high-temperature environment, the MMCs used here should have sufficient stability as well as good mechanical and chemical strength (oxidation). Oxidation occurring at grain boundaries in alloys and at the interface between particle and matrix in MMCs usually increases intergranular fracture, resulting in premature failure and severe brittleness.[8–10] Therefore, in high-temperature applications, it is essential to have a thorough understanding of the oxidation behavior of the aluminum MMCs.

Albite is a candidate ceramic material for high-temperature applications owing to its high melting point, low density, and capacity to retain high strength at elevated temperature. As reinforcements, ceramic particulates can be improved to some extent by reducing the grain size,[11,12] which tends to improve the mechanical properties of the MMCs. Ceramic reinforced aluminum improves fracture toughness and reduces the ductile-to-brittle transition temperature.

S. C. Sharma, Research and Development, Department of Mechanical Engineering, R.V. College of Engineering, Bangalore-560 059, India.

1.1 Kinetic Theory

The data variation of weight change per unit area of the sample due to oxidation (Δm) with time (t) has been investigated to determine the kinetic parameters, namely, the general kinetic constant (k).

The relation between Δm, t, and k is expressed as the linear equation

$$\Delta m = k_l t + c \qquad \text{(Eq1)}$$

The parabolic expression for kinetic oxidation is

$$(\Delta m)^2 = k_p t + c \qquad \text{(Eq2)}$$

Likewise, the cubic expression for kinetic oxidation is given by

$$(\Delta m)^3 = k_c t + c \qquad \text{(Eq3)}$$

Logarithmic relationship is given by

$$\Delta m = k_e \log(at + c) \qquad \text{(Eq4)}$$

And, inverse logarithmic relationship is given by

$$1 / \Delta m = c - k_u \log t \qquad \text{(Eq5)}$$

where k_u, k_e, k_c, k_p, k_l, and c are functional oxidation constants, values of which can be obtained graphically from the slope of the plot. These equations have been used with metal and alloys by many researchers.[13–15]

This article presents the results of a comparative study of the oxidation behavior of aluminum alloy and its MMCs reinforced with albite particles in as-cast and aged conditions. The microstructure and reinforcement of particles were observed using a computer interface with optical microscope.

2. Experimental Procedure

2.1 Material Selection

The present study makes use of the liquid metallurgy technique. A1-6061, which exhibits excellent casting properties and reasonable strength, was used as the base alloy. This alloy is best suited for mass production of lightweight metal castings. The chemical composition of the A16061 alloy is given in Table 1.

Albite is basically a silicate, which is abundantly available. It has a Mohs' hardness of 6 to 6.5, which is nearly equal to that of SiC, which is composed of alumina silicates of sodium. It does not have a sharp melting point but softens at temperatures of 1140 to 1300 °C. The chemical composition of albite particles is given in Table 1.

2.2 Composite Preparation and Aging

Specimens for oxidation tests were prepared using compocasting, with variation of the albite reinforcement in steps of 1, 2, 3, and 4 wt.%, based on the technique described by Mehrabian *et al*.[16] Three aging conditions were selected for oxidation testing. The specimens used to achieve these conditions were subjected to a solution treatment of 10 h at 530 °C followed by quenching in hot water (80 °C). They were aged at room temperature for 12 h, followed[17,18] by aging at 153 °C for 1, 3, and 5 h. The specimens were polished to observe particle distribution by optical microscopy.

2.3 Oxidation Testing Procedure

Specimens for oxidation testing, with dimensions of about $5 \times 8 \times 3$ mm, were polished to 1600 grit finish using a series of emery papers. After rough polishing, the specimen surfaces were polished using 1 μm diamond paste. They were washed in acetone, dried, and weighed before subjecting them to oxidation tests. The tests were performed in a resistance-heating furnace. The specimen plates were hung from a stainless steel net with thin platinum wire. It was exposed in air to temperatures of 500, 600, 700, and 800 K up to a period of 1000 min. Oxidation kinetics was determined by measuring the weight changes/area as a function of time at particular temperature. The oxidized specimens were weighed using electronic balance to an accuracy of 0. 1 mg.

Table 1 Chemical composition of aluminum 6061 alloy and albite by weight percentage

Chemical composition of aluminum 6061 alloy										
Mg	**Si**	**Fe**	**Cu**	**Ti**	**Cr**	**Zn**	**Mn**	**Be**	**V**	**Al**
0.92	0.76	0.28	0.22	0.10	0.07	0.06	0.04	0.003	0.01	Bal.

Chemical composition of reinforcement albite-Na Al Si_3 O_8		
Silica ($6SiO_2$)	**Alumina**	**Soda**
68.7	19.5	11.8

2.4 Energy-Dispersive X-ray, Optical, and Scanning Microscope Observation

The microstructure of sample specimens before and after oxidization was observed by optical microscopy, scanning electron microscopy (SEM), elemental analysis, and oxidized product identification by energy-dispersive X-ray analysis (EDAX). Optical microscopy was used to study the reinforced composites before oxidation to determine the particle distribution, while SEM was used to observe the reinforced composite after oxidation to determine the site of oxidation and morphology of the oxide products formed. Energy-dispersive X-ray analysis was used to identify the structure of the oxide formed.

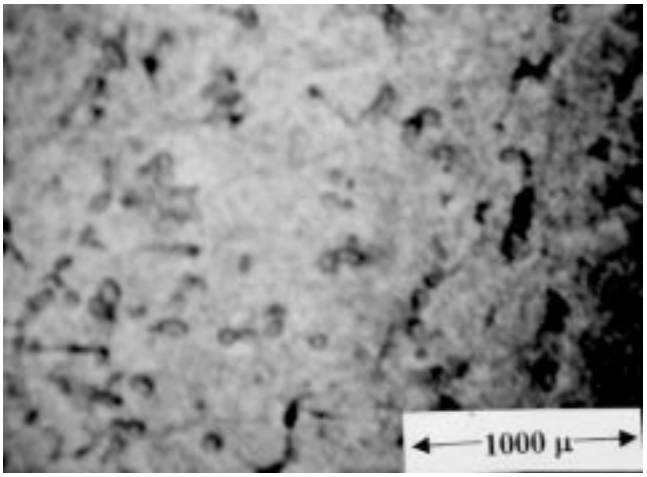

(a)

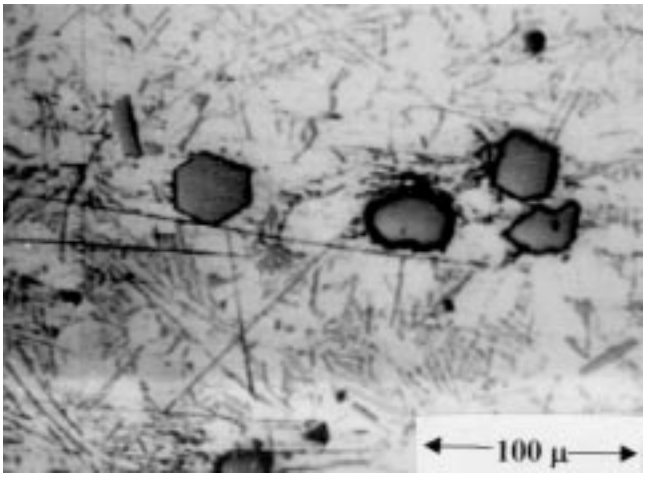

(b)

Fig. 1 (a) and **(b)** Microstructure of A16061/4 wt.%-albite composite

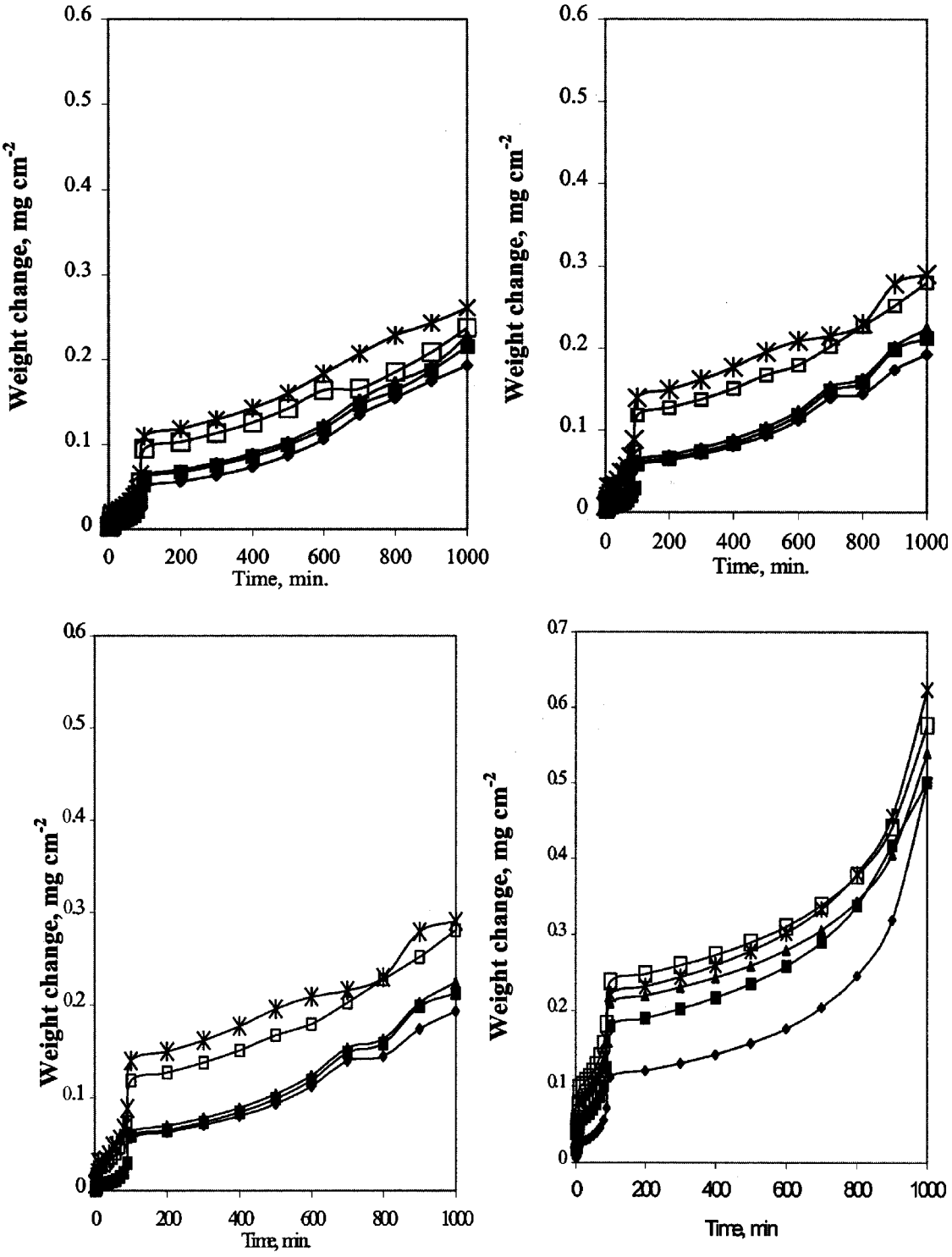

Fig. 2 Kinetics of oxidation of Al/albite MMCs at various temperature: 500, 600, 700, and 800 K

3. Results

The aluminum/albite composites on exposure to hot air (which consists of oxygen, nitrogen, carbon dioxide, nitrogen dioxide, carbon monoxide, nitrogen monoxide, *etc.*) react with these gases to form their respective oxide layers (analyzed by the weight change/area of the specimens against oxidation time). After the oxidation test, a thin external oxide scale was formed in hot atmosphere.

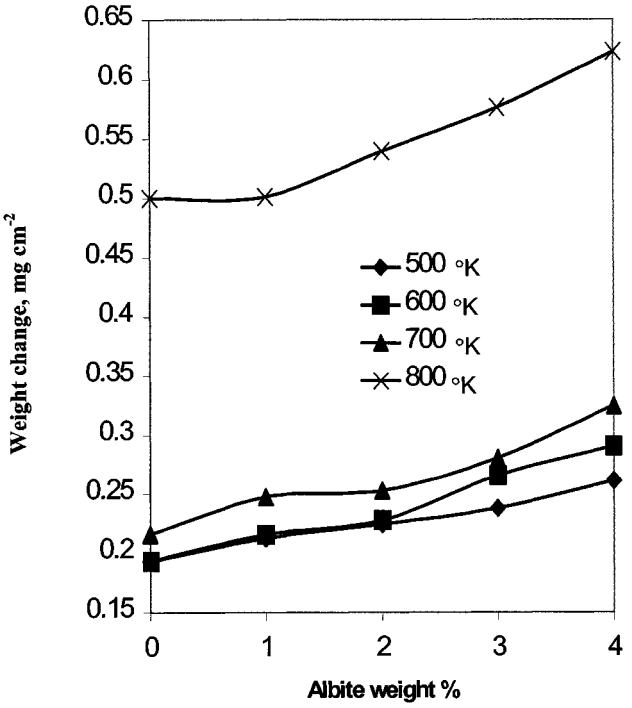

Fig. 3 Weight change/area due to oxidation of Al/albite MMCs vs different percentages at 1000 min

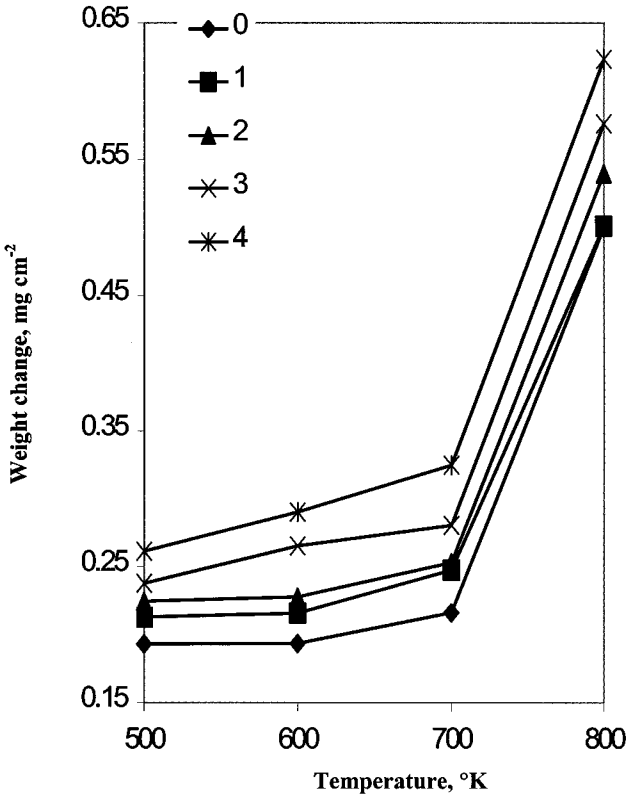

Fig. 4 Weight change/area due to oxidation of Al/albite MMCs vs different temperatures at 1000 min

3.1 Microstructure of the Composites

Samples for microscopic examinations were prepared by standard metallographic procedures, etched with Keller's agent, and examined under optical microscope. Optical microstructure of the die-cast aluminum-albite particle composite is shown in Fig. 1. The particles were of irregular shape of approximately 90 to 150 μ size. They demonstrate that uniform distribution of reinforcements can exist, which show good bonding between the reinforcement and matrix alloy.

3.2 Effect of Exposure Time

Aluminum alloys and MMCs play a most significant role as construction materials for elevated temperature applications, especially in atmospheres containing nascent oxygen (*e.g.*, the LEO: low earth orbits of satellites). This investigation evaluates the growth mechanism of the-oxide coating. Figure 2 shows the variation of weight change/area in Al_2O_3 with time at different temperatures between 500 and 800 K with constant step length of 100 K. The oxidation behavior of the matrix is found to be similar to that of MMCs (similar rate at a given temperature).

3.3 Effect of Reinforcement

Figure 3 shows the variation of weight change/area versus weight percentage of reinforcement. As indicated, the weight change/area increases monotonically with increase in percentage of reinforcement.

3.4 Effect of Temperature

Figure 4 shows the variation of weight change/area versus oxidation time in air. Both the unreinforced and reinforced materials have almost similar oxidation kinetics at all temperatures. Figure 4 also shows weight change/area versus temperature, in which the weight change/area increases monotonically with an increase in temperature up to 700 K. The extent of reaction increased as the temperature of oxidation was increased to 700 K. The figure reveals that oxidation of both the reinforced and unreinforced alloy maintains the same trend up to 700 K. With further change in temperature, the oxidation weight change/area changes. This temperature is known as the transition temperature (700 K).

3.5 Effect of Aging

The results in Fig. 5 show that in both as-cast and aging environments, the 1, 3, and 5 h oxidation kinetics decreased significantly, irrespective of the albite particulate content. The duration of aging seems to be of little significance. It is evident from the graph that aging for a 1 h duration causes the oxidation kinetics to drop drastically. On further aging for 3 and 5 h, specimens showed a marginal increase in resistance to oxidation, over 1 h aging.

4. Discussion

The effect of exposure time on oxidation kinetics curves is shown in Fig. 2. The oxidation kinetics exhibits a sigmoid pat-

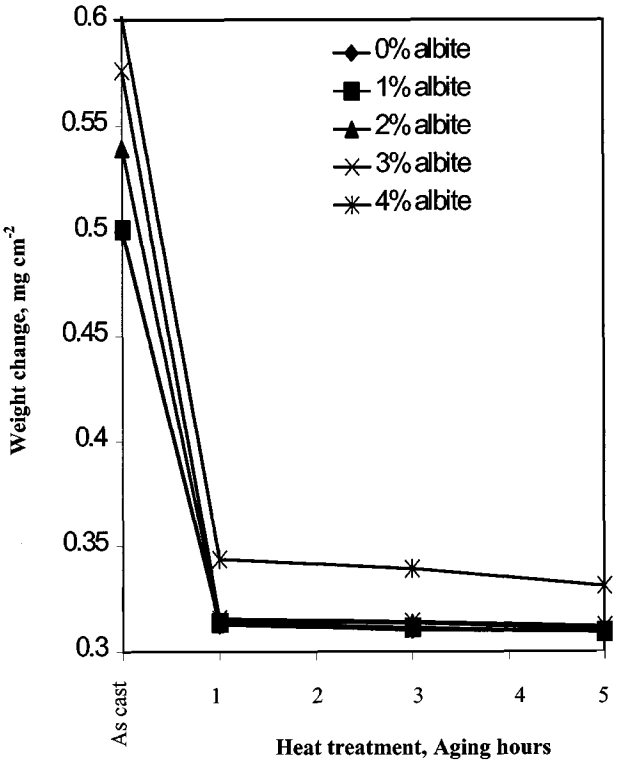

Fig. 5 Weight change/area due to oxidation of Al/albite MMCs vs different aging times at 1000 min with 800 K

tern, which subsequently changes to a linear pattern. The initial pattern of oxidation is characterized by predominant formation of Al_2O_3, which is a strong protective layer. But due to the difference in the coefficient of thermal expansion of the matrix and Al_2O_3, the metal tries to expand more than that of the Al_2O_3 layer as temperature changes. Due to thermal mismatch, there is a possibility of cracks generated in the Al_2O_3 layer. Upon cracking, oxygen reacts with the exposed metal and secondary oxidation takes place. The secondary oxidation continues until the oxide layer covers the exposed surface. Both SEM (Fig. 6) and EDAX (Fig. 7) offer clear evidence of cracks on the Al_2O_3 layer.

The effect of albite particle on oxidation kinetics is shown in Fig. 3. The interfacial region was characterized by a high dislocation density arising from differential thermal contraction during cooling.[19,20] The high strain energy associated with dislocations may have enhanced the site initiation process when the specimens were exposed to hot environments. Oxidation reactions have dominated at this interface formed between the reinforced particle and matrix alloy. The composites having larger concentration of reinforcement have larger sites, which promotes oxidization, resulting in the formation of thicker oxidation scales on the matrix material. Thus, a larger weight change/area is observed due to thick oxide scale formation on the specimen, as shown by SEM (Fig. 8).

The effect of temperature on oxidation kinetics is shown in Fig. 4, which indicates that cracking of thermally produced Al_2O_3 layers allows oxygen to diffuse along the grain boundaries in the form of oxygen ions. Aluminum exposed to the oxidizing environment starts to react, which increases with the amount of cracking of Al_2O_3 layer produced, as shown by SEM (Fig. 6). For this reason, there is a possibility of intermolecular oxidation as the alloy and MMC temperature attained is close to the recrystallization temperature. The transition temperature is the same for both alloys and MMCs. This shows that there is no chemical reaction between the alloy and reinforcement.

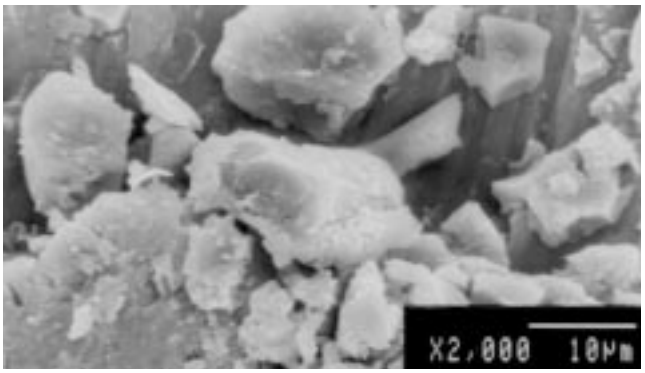

Fig. 6 SEM photograph showing cracks on the Al_2O_3 layer

The effect of aging time on oxidation kinetics curves is shown in Fig. 5. Improvement in the oxidation resistance of the composites may be due to the possibility of formation of a protective layer of aluminum oxide (Al_2O_3) on the specimen due to aging, which acts as a protective layer against oxidation at the initial stage. A variation in density of MMCs can be attributed to the annihilation factor of the lattice defect by aging (above recrystallization temperature), which results in an improved homogeneous nature of composites,[21] which increases the oxidation resistance of MMCs. By aging, there is a possibility of occurrence of plastic yielding, which could relieve residual stresses[22] in the composite specimens, reducing mismatch strain, which may be one of the reasons for the increase in oxidation resistance of both the alloy and the MMCs. Aging forms an intermetallic precipitate between the interface of the matrix and reinforcement,[23] which improves the oxidation resistance properties of alloys.

5. Conclusions

- The interface between the reinforcement and the matrix was the main site for nucleation of oxidation.
- Oxidation weight change/area increases rapidly at the initial stage but remains constant at later stages.
- Oxidation weight change/area shows only a moderate increase with increase in reinforcement content.
- In albite reinforced composites, albite enhances the reactive nature of the matrix alloy at higher temperatures.
- The Al_2O_3 layer growth increases with the increase in exposure time.
- The oxidation kinetics is strongly dependent on the heat treatment conditions. Upon heat treatment, both the matrix and the composite exhibit greater oxidation resistance, which

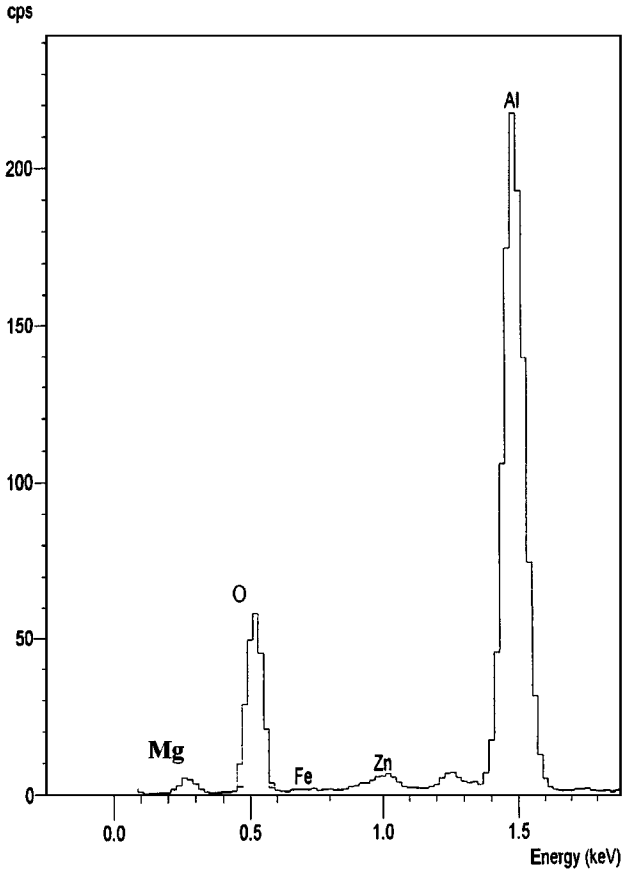

Fig. 7 EDAX graph showing evidence of the presence of Al_2O_3 from subscale after oxidation at 800 K

may be attributed to stress relaxation at the matrix-particle interface and propagation of dislocation.

References

1. S. Elomari, R. Boukhili, and M.D. Skibo: *J. Mater. Sci.*, 1995, vol. 30, p. 3037.
2. Metal Matrix Composites, J.N. Fridlymander: Chapman and Hall, Oxford, United Kingdom, 1995.
3. H. Jones, C.A. Lavender, and M.T. Smith: Scripta Metall., 1987, vol. 21, p. 1565.
4. S.C. Sharma, B.M. Girish, R. Kamath, and B.M. Satish: J. Mater. Eng. Performance, 1999, vol. 8, p. 1999.
5. E.A. Feest: Mater. Des., 1986, vol. 7, p. 58.
6. John E. Allison and Gerald S. Cole: J. Met., 1993, vol. 45, p. 29.

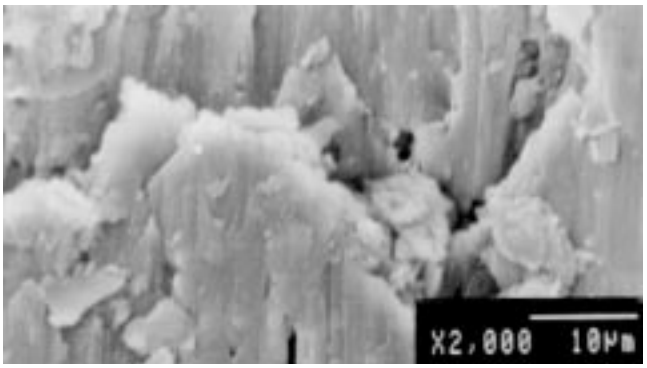

Fig. 8 SEM photograph showing thick aluminum oxide scale

7. R.R. Bowles, D.L. Macini, and M.W. Toaz: *Advanced Composites—The Latest Developments*, Proc. 2nd Conf. on Advanced Composites, Peter Beardmore and Carl F. Johnson, eds., ASTM International, Minnesota, MI, 1990, p. 21.
8. Z. Rizhan, G. Manjiou, and Z. Yu: Oxid. Met., 1987, vol. 27, p. 253.
9. R.H. Brincknell and D.A. Woodford: Metall. Trans. A, 1981, vol. 12A, p. 1673.
10. D.A. Woodford and R.H. Bricknell: Metall. Tran. A, 1981, vol. 12A, p. 2467.
11. S. Ruess and H. Vehoff: Scripta Metall. Mater., 1990, vol. 24, p. 1021.
12. K.S. Min, A.J. Ardell, S.J. Eck, and F.C. Chen: J. Mater. Sci., 1995, vol. 30, p. 5479.
13. R. Mitra and V.V. Rama Rao: Metall. Mater. Trans. A, 1988, vol. 29A, p. 1665.
14. T. Tanabe, M. Nishiura, and Z. Asaki: Mater. Trans., JIM, 1992, vol. 33(12), p. 1155.
15. R. Mitra, V.V. Rama Rao, and Y.R. Mahajan: Mater. Sci. Technol., 1997, vol. 13, p. 415.
16. R. Mehrabian, R.G. Rick, and M.C. Flemings: Metall. Trans., 1974, vol. 5, pp. 1899–1905.
17. M. Gupth and M. Manoharan: Mater. Sci. Technol., 1997, vol. 13, p. 523.
18. S. Suresh, T. Christman, and Y. Sugimum, Scripta Metall., 1989, vol. 23(9), p. 1599.
19. Z. Trojanova, M. Pahutova, J. Kiehn, P. Lukac, K.U. Kainer: Proc. 1st Int. Conf., San Sebastian, Spain, Sept. 1996, p. 1001.
20. B. Budiansky, J.W. Hutchinson, and J.C. Lambropoulos: Int. J. Solids Struct., 1983, vol. 19, p. 337.
21. S.K. Prasad, A.K. Patwardhan, and A.H. Yegneswaran: J. Mater. Sci., 1996, vol. 31, p. 6317.
22. Rajendra U. Vaidya and K.K. Chawla: Comp. Sci. Technol., 1994, vol. 50, p. 13.
23. Y. Song, and T.N. Bakes: Mater. Sci. Technol., 1994, vol. 10, p. 406.